doi: 10.1111/j.1365-3121.2010.00928.x

Late Quaternary folding in the Jura Mountains: evidence from syn-erosional deformation of fluvial meanders

Herfried Madritsch,[1,2] Frank Preusser,[3] Olivier Fabbri,[2] Vincent Bichet,[2] Fritz Schlunegger[3] and Stefan M. Schmid[1]

[1]*Institute of Geology and Paleontology, Universität Basel, 4056 Basel, Switzerland;* [2]*UMR 6249 Chrono-Environnement, Université de Franche-Comté, 25030 Besancon Cedex, France;* [3]*Institute of Geological Sciences, Universität Bern, 3012 Bern, Switzerland*

ABSTRACT

The present tectonic activity of the Jura fold-and-thrust belt is a matter of scientific debate. At its north-western front, differentially uplifted palaeo-meanders of the Doubs River record Late Quaternary growth of the Citadelle Anticline, associated with a minimum rock uplift of 13 m. Local rock uplift rates estimated from optical stimulated luminescence dating of oxbow lake deposits measure 0.17 ± 0.05 mm per annum. Reconstruction of the deformation history reveals that buckling took place simultaneously with focused Pleistocene river incision. The structural, geomorphic and temporal setting suggests that active deformation could possibly be sustained by incision-related erosion. These observations shed new light on the modes of recent deformation in the Jura Mountains and on the present-day dynamics of the Alpine orogenic front.

Terra Nova, 22, 147–154, 2010

Introduction

The Jura Mountains represent the most external deformation front of the European Alps (Figs 1 and 2). This arcuate range is considered as a textbook example of a thin-skinned foreland fold-and-thrust belt the formation of which is widely accepted to have resulted from 'distant push' (Laubscher, 1961; Burkhard and Sommaruga, 1998; Willett and Schlunegger, 2009). Late Miocene crustal shortening in the external crystalline massifs of the Central Alps induced large-scale decoupling of the Mesozoic sedimentary cover along a sole thrust in Middle to Late Triassic evaporites ('décollement'; Fig. 2).

The main tectonic structures of the Jura Mountains formed during a short-lived event. In the outermost northern parts of the range, it is inferred to have lasted from the Late Miocene to Early Pliocene times (Becker, 2000). Post-Early Pliocene tectonic activity is characterized by very low deformation rates and is still ill-defined (Meyer *et al.*, 1994; Nivière and Winter, 2000; Giamboni *et al.*, 2004a). Herein, we present geomorphic evidence for Late Quaternary folding at the north-western front of the belt, estimate rates of associated rock uplift and discuss the geodynamic implications of these findings.

Correspondence: Herfried Madritsch, Nagra, Hardstrasse 73, Wettingen 5430, Switzerland. Tel.: +41 56 437 12 49; e-mail: herfried.madritsch@nagra.ch

Structural and geomorphic setting

The study area is located within the Besançon Zone, the most external segment of the Jura belt that was thrusted onto the pre-existing Eo-Oligocene intracontinental Rhine-Bresse Transfer Zone (Madritsch *et al.*, 2008; Fig. 1). The southern boundary of the Besançon Zone is formed by a 100-km-long thrust zone called Faisceau Bisontin (Chauve *et al.*, 1980; FB in Figs 1 and 2).

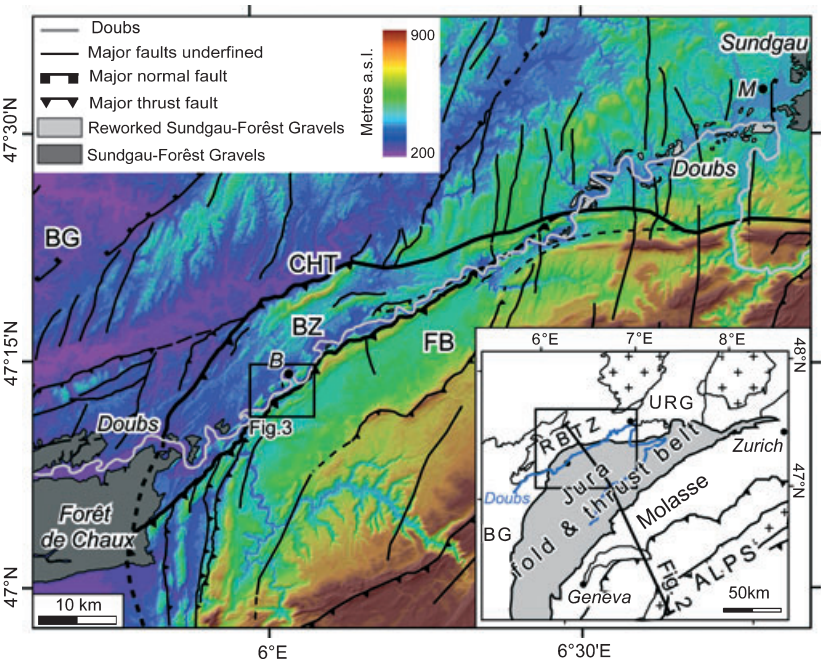

Fig. 1 Shaded digital elevation model of the north-western Jura fold-and-thrust belt (50-m horizontal resolution). Note the course of the Doubs River that incises parallel to the Faisceau Bisontin thrust zone and the location of the study area (see Fig. 3). B, Besançon; BG, Bresse Graben; CHT, Chailluz Thrust; FB, Faisceau Bisontin; M, Montbéliard; RBTZ, Rhine-Bresse Transfer Zone; URG, Upper Rhine Graben.

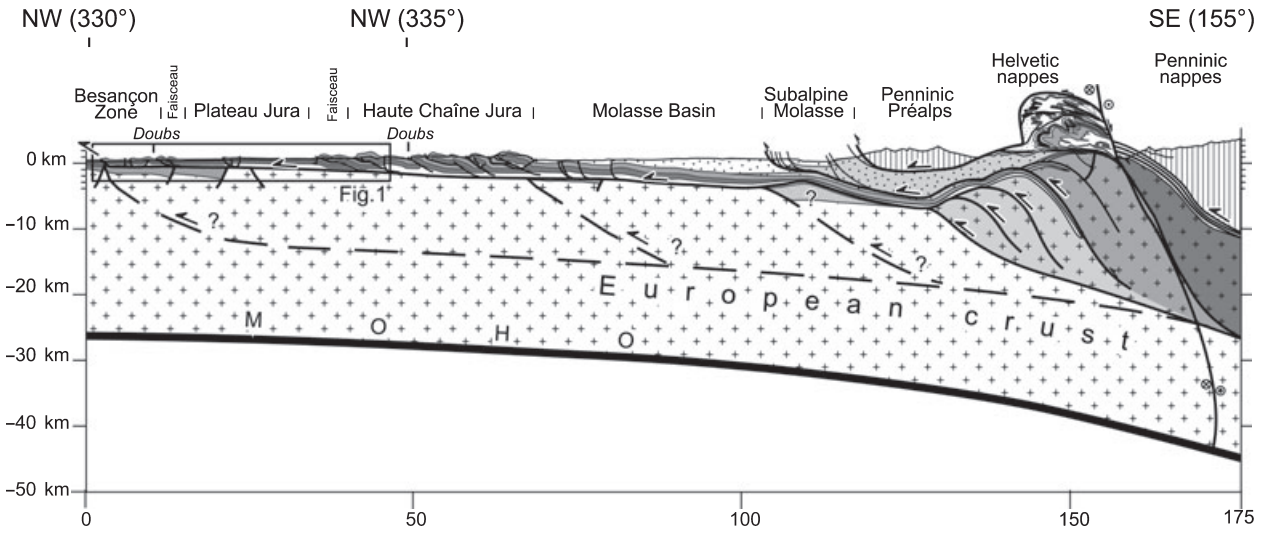

Fig. 2 Simplified cross-section across Central Alps, Molasse Basin and Jura fold-and-thrust belt (modified after Burkhard and Sommaruga, 1998). The décollement horizon of the thin-skinned Jura fold-and-thrust belt (thick solid line) is located in Triassic evaporites and rooted in the Central Alps. Suspected basement faults dissecting the European crust are given as thick dashed lines (see text for discussion).

The Citadelle Anticline is located immediately to the NW of this thrust zone (Figs 1 and 3). It has a clear topographic expression with a surface length of 15 km and is characterized by a gently double plunging ENE–WSW striking axis. Field evidence for bedding-parallel slip indicates that the Citadelle Anticline formed by flexural-slip folding. Buckling of the competent Middle to Late Jurassic limestones forming the fold limbs is compensated by plastic deformation of Triassic evaporites and Early Jurassic marls in the core of the anticline (Fig. 4a). Palaeostress analysis of fault–slip pairs indicates that folding was induced by NW–SE-oriented compression (Madritsch *et al.*, 2008), i.e. perpendicular to the fold axis and parallel to the present-day orientation of maximum horizontal stress measured *in situ* nearby (Becker, 2000).

The Citadelle Anticline is repeatedly crossed by the highly sinuous Doubs River. The lower reach of the river valley runs roughly parallel to the FB thrust zone (Fig. 1). It developed from the Late Pliocene onwards, i.e. since the early Doubs occupied the peniplane of the Palaeo-Aare, which deposited the Middle Pliocene Sundgau-Forêt de Chaux (SFC) Gravels (Fig. 1) before being deflected into the Rhine Graben at about 2.9 Ma (Petit *et al.*, 1996; Ziegler and Fraefel, 2009). During its Late Pliocene to present evolution, the Doubs degraded the SFC gravel plain and incised into the underlying Jurassic bedrock, carving out a narrow canyon (Madritsch *et al.*, 2009; Fig. 1). Strath-terraces, wind gaps and three distinctive palaeo-meanders were cut into the Citadelle Anticline during this incision phase.

The highest remnants of fluvial deposits detected along the anticline are located 110 m above the active Doubs channel in the Chaudanne wind gap (CH in Fig. 3). Pebble petrography and heavy mineral spectra of these deposits reveal an Alpine provenance, indicating that they represent reworked SFC Gravels (Madritsch *et al.*, 2009). Thus, the minimum deposition age of these gravels (2.9 Ma; Petit *et al.*, 1996; Fejfar *et al.*, 1998) represents the maximum age of the Chaudanne wind gap. The palaeo-meander of Velotte (VEL) is located 60 m below the wind gap (Fig. 4b), and hence, must be younger. The Malcombe (MAC) and Roche d'Or (RDO) palaeo-meanders are located further west at still lower elevations (Fig. 3). Most intriguingly, the present-day surface elevation of the more distal MAC palaeo-meander is lower (9 m above the Doubs) relative to that of the more proximal RDO palaeo-meander (18 m) located on the crest of the anticline. This observation led to the hypothesis that the RDO palaeo-meander could have been uplifted along the fold axis with respect to the distal MAC palaeo-meander (Dreyfuss and Glangeaud, 1950).

To test this hypothesis and to potentially quantify Quaternary fold-growth along the Citadelle Anticline, we performed high-precision geodetic levelling and geoelectric subsurface imaging to determine the bedrock elevation of the meander channels. Optical stimulated luminescence (OSL) was carried out to date the deposits that filled up the abandoned channels.

Methods

Geodetic levelling was performed using a PRO XRS Trimble GPS and Trimble GPS Pathfinder software (Trimble, Sunnyvale, CA, USA). Measurements were taken at 52 sites along a profile from the presently active Doubs River channel across the Roche d'Or and Malcombe palaeo-meanders (Fig. 5). The field data were treated with reference to the DGPS station of the Besançon Observatory located 6 km north of the study area resulting in a measurement precision of at least ± 10 cm.

Geoelectric resistivity profiles were acquired using a multi-electrode dipole–dipole array (IRIS Instruments

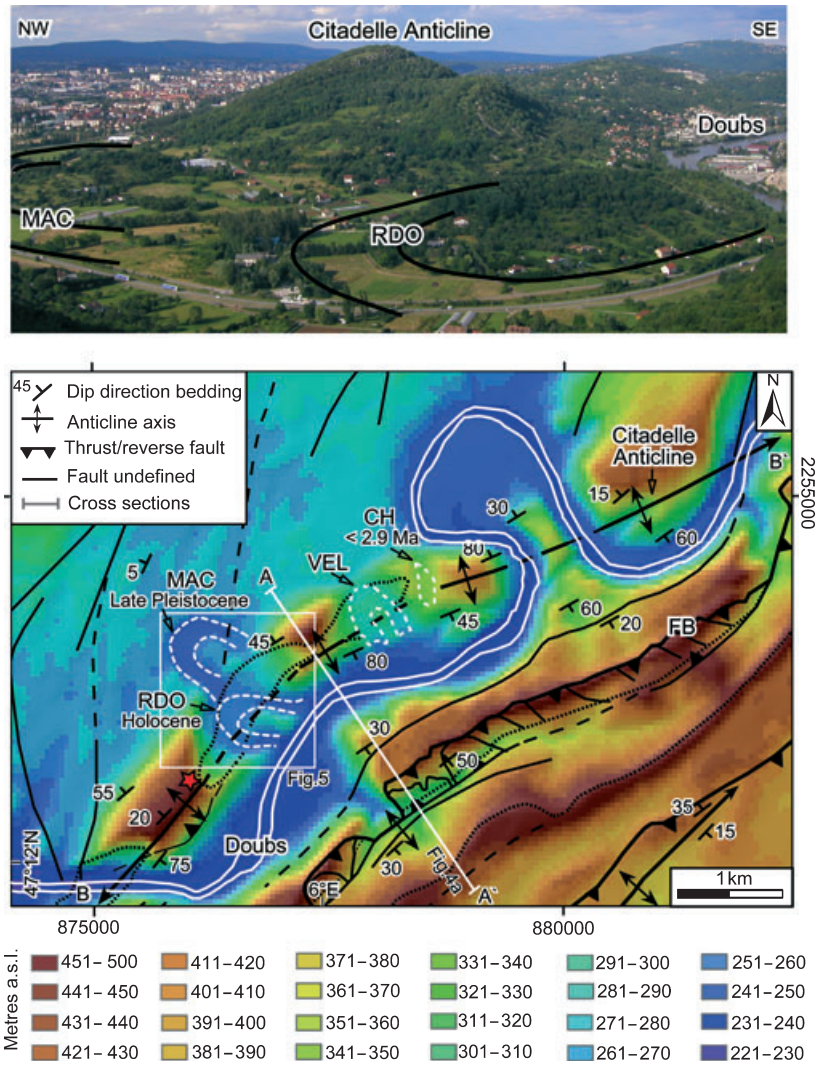

Fig. 3 Shaded digital elevation model of the study area showing the Citadelle Anticline and the palaeo-meanders. Pleistocene growth of the Citadelle Anticline led to a cut-off of the Malcombe (MAC) and subsequent relative rock uplift of the Roche d'Or (RDO) palaeo-meander. Further palaeo-topographic markers are the Velotte palaeo-meander (VEL) and the Chaudanne wind gap (CH). The stippled line marks the boundary between outcrops of Middle Jurassic limestones that form the limbs of the anticline and Early Jurassic marls that outcrop in its core. Note the positions of two cross-sections A–A′ and B–B′ shown in Fig. 4. The red star marks the location at which the photograph was taken (view towards NE).

SYSCAL R1, 36 electrodes, electrode spacing 1.5–5 m). Data were treated using the RES2DINV software (Locke and Barker, 1995) to obtain resistivity pseudo-sections (Fig. 6). The pseudo-sections were interpreted by correlation with geological logs from nearby wells (Fig. 7).

Samples for OSL dating were obtained from four trenches dug into sedimentary fill of the MAC and RDO palaeo-meanders (Fig. 8). From each trench, two samples were taken at a depth of 135–150 cm. Homogeneous silts were excavated below a soil and sediment cover of 80–100 cm thickness at all sites. Determination of the palaeo-dose (D_e) was carried out on fine-grained quartz separates (Mauz and Lang, 2004) using the single-aliquot regenerative dose (SAR) protocol. Standard tests were performed to identify appropriate measurement conditions (Wintle and Murray, 2006). A pre-heat of 230 °C for 10 s was applied prior to all OSL measurements (60 s at 125 °C). The samples revealed very good luminescence properties in the standard tests (< 1% recuperation, recycling ratios within 5% of unity). Present-day moisture was measured in all samples. Average water content of 15–25% was assumed for the sediments, accounting for possible changes in the past hydrological conditions. Age calculation was carried out using the ADELE software (Kulig, 2005) considering geographical position and sediment overburden for estimating the contribution by cosmic rays to the total dose rate.

Results

Geodetic levelling shows a gentle slope between the lower-lying surface of the distal MAC palaeo-meander and the higher surface of the proximal RDO palaeo-meander and yields no distinctive scarp. The surface of both palaeo-meander channels is horizontal, resembling a juvenile alluvial plain (Fig. 9). The slope from the RDO meander towards the present Doubs valley is steeper and features a convex break that probably represents a young strath terrace.

The geoelectric resistivity profiles shown in Fig. 6 are oriented perpendicular to the channel axis of the MAC and RDO palaeo-meanders (Fig. 5). The contact between the low electrical resistivity, groundwater-saturated alluvial sediments and the underlying bedrock that shows significantly higher resistivity forms a strong geophysical contrast, which allowed determining the bedrock elevation of the palaeo-meanders across the resistivity pseudo-sections (Fig. 6). In section I across the MAC palaeo-meander (Fig. 6a), the maximum bedrock depth was found at 234 m a.s.l. In section II crossing the RDO palaeo-meander (Fig. 6b), it is at ~247 m a.s.l., hence 13 m higher than the channel base of the MAC palaeo-meander.

The silt sediments sampled for OSL dating revealed very little to no carbonate content, which excludes a colluvial sediment source from the slopes of the meander arms composed of limestones and calcareous marls. Most likely, the sampled deposits represent the filling of an oxbow lake that formed after the meander channels were abandoned and correspond to

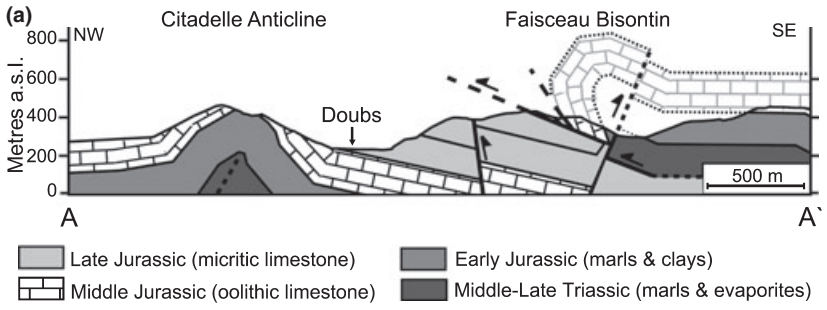

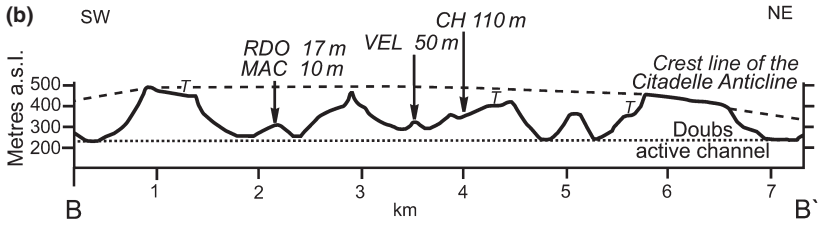

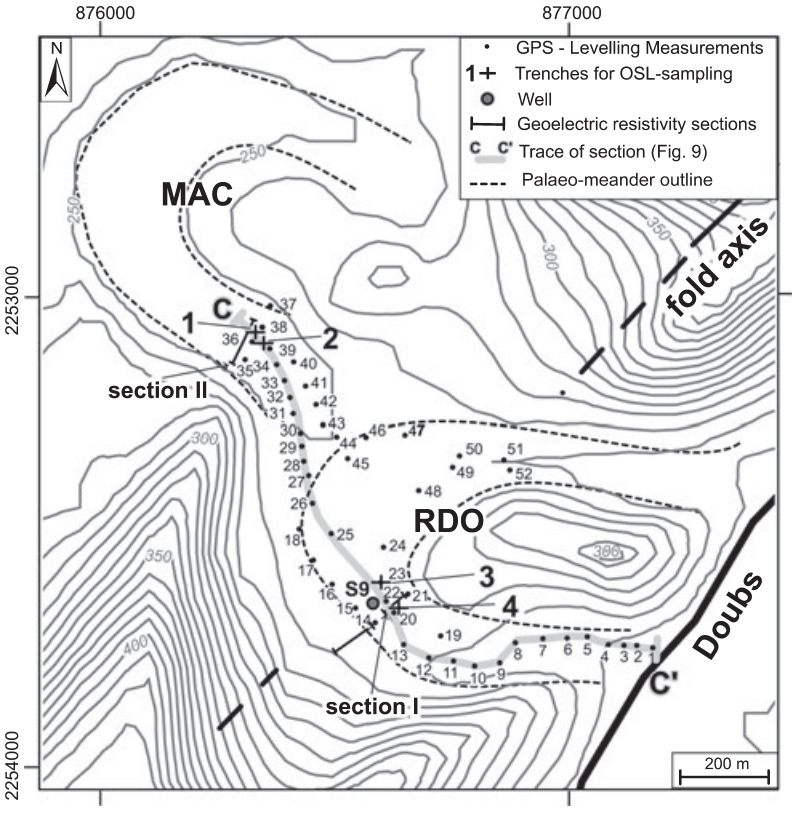

Fig. 5 Topographic map of the Roche d'Or (RDO) and Malcombe (MAC) palaeo-meanders (see Fig. 3) showing the locations of: geodetic levelling points, geoelectric resistivity profiles I and II (see Fig. 6), well S9 (see log in Fig. 7), trenches 1–4 dug for OSL sampling (see Fig. 8) and the trace of the topographic section C–C′ given in Fig. 9. The numbers attached to the levelling points are given in Table S1. The stippled line provides the outlines of the Malcombe (MAC) and Roche d'Or (RDO) palaeo-meanders.

the upper alluvial sequence revealed by well S9 (Fig. 7). Samples from the MAC palaeo-meander yielded OSL ages of 33 ± 2 and 27 ± 2 ka in Trench 1. However, 63 ± 4 and 96 ± 7 ka were obtained in Trench 2 (Figs 5 and 8, Table 1). The latter ages are neither internally consistent nor do they agree with those obtained in Trench 1. The problem may be that Trench 2 samples were taken with poor stratigraphic control from the bottom of the exposed profile. Most likely, old sediment from the bottom of the oxbow lake was included during sampling and we consequently assume that the ages from the Trench 1 samples (mean 30 ± 5 ka) do more likely represent the time when the oxbow lake was filled. These ages correlate with the end of the Middle Late Pleistocene, a period with relatively temperate climatic conditions in Central Europe (Preusser, 2004). All OSL ages for the RDO palaeo-meander indicate deposition during the Middle Holocene (Trench 3: 8.2 ± 0.5, 6.6 ± 0.4 ka; Trench 4: 4.8 ± 0.3, 4.8 ± 0.3 ka; Fig. 8, Table 1), a significantly younger age compared with that of the more distal but lower-lying MAC palaeo-meander.

Fig. 4 (a) Geological section across the Citadelle Anticline and the Faisceau Bisontin thrust zone (see Fig. 3 for location). (b) Topographic cross-section along the crest of the Citadelle Anticline, parallel to its fold axis mapped in Fig. 3, illustrating strath terraces, wind gaps and palaeo-meanders that were cut into the fold during Pleistocene incision of the Doubs River. The dashed grey line marks the trend of the double plunging fold crest line that culminates in the area of the deepest incision. CH, Chaudanne wind gap; MAC, Malcombe palaeo-meander; RDO, Roche d'Or palaeo-meander; VEL, Velotte palaeo-meander; T, Strath terrace, interpreted.

Discussion

This study indicates an inversion of the palaeo-meander sequence preserved across the Citadelle Anticline (Figs 3 and 9). The younger RDO palaeo-meander, located on the crest of the anticline has been uplifted with respect to the older MAC palaeo-meander located on the fold limb.

Buckling under consistent NW–SE horizontal compression occurred simultaneously with river incision since at least 2.9 Ma. This is evident from the comparison of palaeo- and recent stress orientations (Madritsch *et al.*, 2008), the presence of reworked

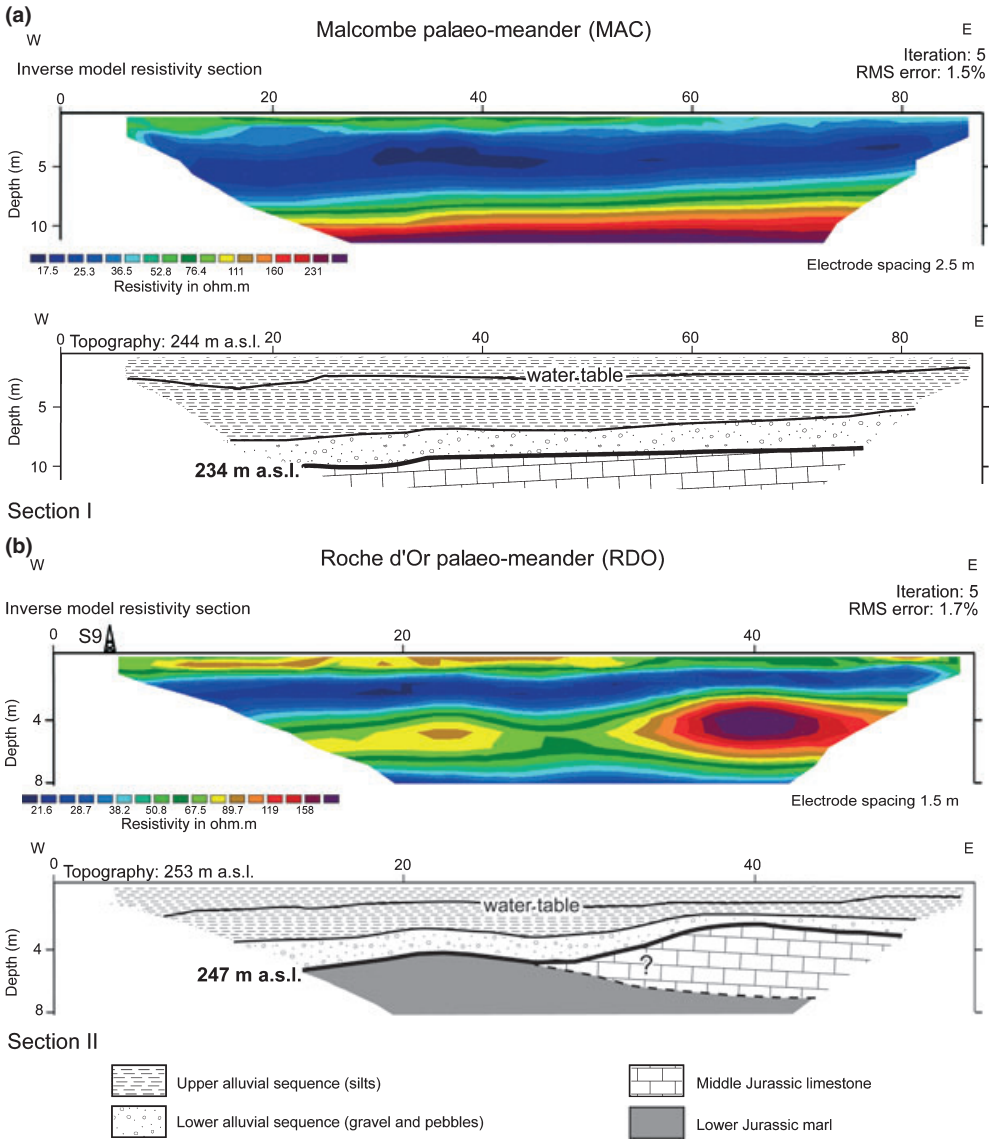

Fig. 6 Electrical resistivity profiles across the Roche d'Or and Malcombe palaeo-meanders (see Fig. 5 for locations) and interpretations based on geological logs from nearby wells (simplified stratigraphy, compare with Fig. 7). The good correspondence between the depths suggested by the electrical profile inversion results and those shown by the geological logs indicates that the error margin on the estimates of the alluvium–bedrock interface depth does not exceed ±0.5 m. Note the difference in vertical scales between the two sections and the elevation a.s.l. of topography and the alluvium–bedrock interface given in thick letters.

Middle Pliocene SFC Gravels in the Chaudanne wind gap, the formation of the Velotte palaeo-meander and most importantly, the syn-erosional differential uplift between the MAC and RDO palaeo-meanders. Incision was structurally guided once the river became locked between the Citadelle Anticline and the Faisceau Bisontin thrust zone (Fig. 4a) and further facilitated after it had reached the marls within the core of the anticline (stippled line in Fig. 3). At present, the culmination of the fold crest coincides with the area of strongest erosion where the ancient and recent courses of the river repeatedly cross the anticline perpendicular to the fold axis (Fig. 4b). This geomorphic scenario provokes the question whether the continuous erosional unloading of the fold structure by the Doubs may have influenced the localization of sustained Quaternary deformation, a positive feedback proposed by numerical models linking deformation and surface processes (Simpson, 2004; Zeilinger *et al.*, 2005).

As folding and erosion by river incision occurred simultaneously, precise deformation quantification is hindered. The detected bedrock elevation difference of 13 m between the two palaeo-meanders (Fig. 9) also contains a non-quantifiable erosive component and thus reflects the minimum

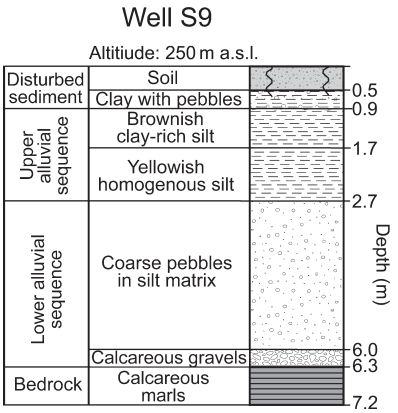

Fig. 7 Geological log of well S9 (see Fig. 5 for location) used for the interpretation of the geoelectric resistivity sections. The bedrock reached by this well is composed of Jurassic calcareous marl. It is overlain by a lower sequence of alluvial deposits consisting of calcareous gravels and silts with embedded pebbles and followed by an upper alluvial sequence of homogeneous clay-rich silt [Source: French Bureau de Recherches Géologiques et Minières (BRGM, weblink: http://infoterre.brgm.fr/)].

relative rock uplift related to crustal deformation. Deformation rates are difficult to constrain, as the acquired ages only represent the time when the meanders were abandoned and filled, not necessarily the time during which they became deformed. However, the observation that deformation and incision occurred synchronously justifies the assumption that the cut-off of the MAC meander was partly caused by the tectonic uplift along the Citadelle Anticline. At present, the dated MAC deposits are located roughly 5 ± 0.5 m below the bedrock surface of the RDO palaeo-channel (Fig. 9). We thus infer that a minimum rock uplift of 5 m occurred since sediment deposition and filling of the MAC palaeo-meander (30 ± 5 ka). This corresponds to a local Late Pleistocene rock uplift rate estimation of 0.17 ± 0.05 mm per annum. This rough estimation is higher than the Latest Pliocene to recent 0.05 mm per annum uplift rate determined from regional palaeo-topographic reconstructions (Madritsch *et al.*, 2009), but is similar to estimates from neighbouring areas (Nivière *et al.*, 2006).

In contrast to previous studies, reporting late-stage deformation only outside the thin-skinned Jura fold-and-thrust belt proper (Nivière and Winter, 2000; Giamboni *et al.*, 2004b), Late Quaternary deformation along the Citadelle Anticline occurs within the belt (Fig. 1), presumably by buckling. This implies that Quaternary shortening of the Mesozoic cover sequence is decoupled from the basement at least on a local scale, i.e. over the scale of the profile in Fig 4a. Thus, present-day activity of the thin-skinned Jura fold-and-thrust belt, an activity related to ongoing shortening within the Central Alps, cannot be entirely excluded. However, epicentral depths of earthquakes in the north-western foreland are mostly below the presumed thin-skinned décollement horizon (Kastrup *et al.,* 2004; Schmid and Slejko, 2009). This suggests that recent foreland tectonics are most likely no longer thin-skinned in the sense of the distant push theory (Laubscher, 1961), but involve late-stage thick-skinned basement deformation, probably reflecting a northward propagation of the Alpine deformation front in depth (Guéllec *et al.*, 1990; Meyer *et al.*, 1994; Pfiffner *et al.*, 1997; Mosar, 1999; Ustaszewski and Schmid, 2007; Fig. 2).

Conclusion

On the basis of our observations and the geodynamic considerations outlined above, we conclude that the Mesozoic sequence of the Jura Mountains is still undergoing shortening along the evaporitic décollement horizon of the foreland fold-and-thrust belt. In contrast to the Neogene thin-skinned development of the belt, active thrusting is most likely rooted in the nearby basement.

Such basement deformation may lead to local decoupling between basement and cover and reactivation of structures that initially formed during the thin-skinned Jura deformation period as is likely the case for the Citadelle Anticline. As a consequence, the tectonics of the north-western Alpine foreland are characterized by the superposition of shallow, – apparently largely aseismic – deformation of the Mesozoic cover and seismogenic faulting within the underlying basement. The question whether erosion could possibly be responsible for the localization of renewed out-of-sequence activity within the formerly thin-skinned fold-and-thrust belt remains to be answered.

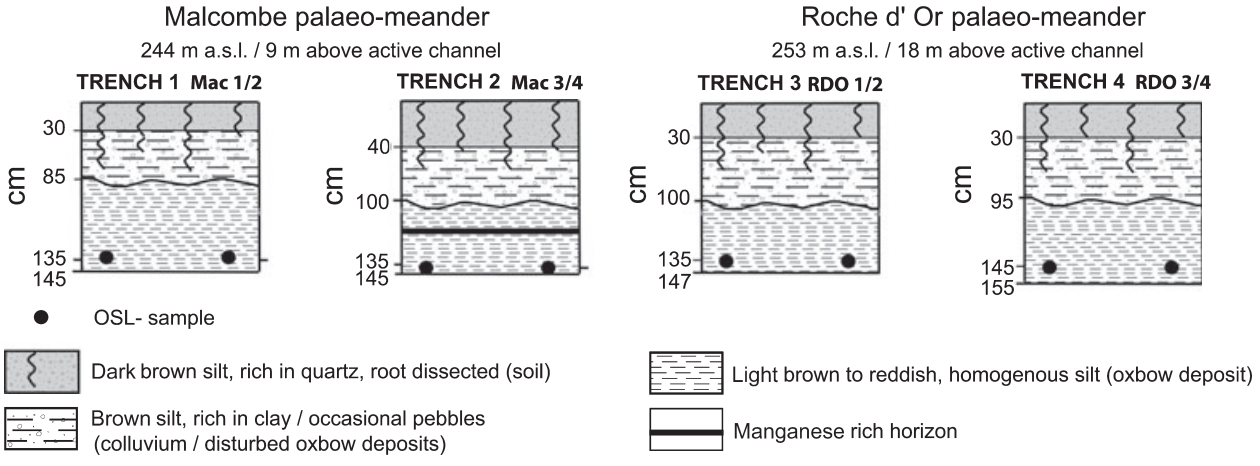

Fig. 8 Geological logs of trenches 1–4 from which the OSL-samples were taken (see Fig. 5 for locations). Note that the sampled silts correlate with the upper alluvial sequence as revealed by well S9 (Fig. 7).

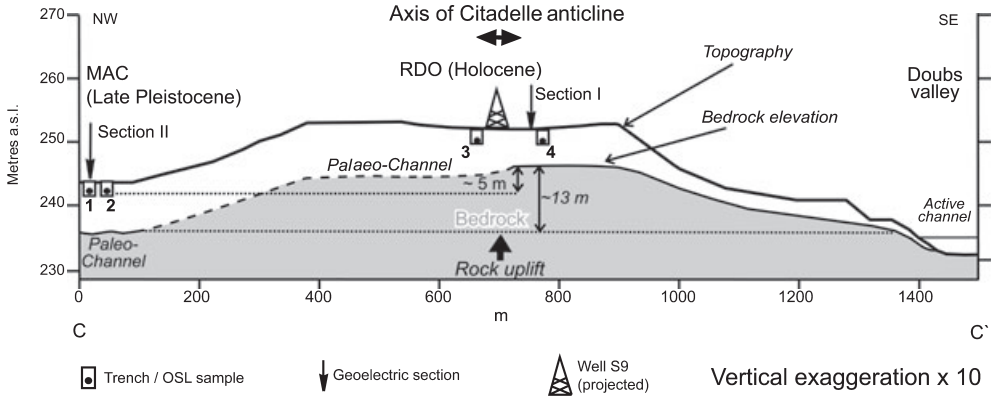

Fig. 9 Vertically exaggerated topographic profile (see Fig. 5 for location) across the Roche d'Or and Malcombe palaeo-meanders as constrained by the results of this study. The locations of the geoelectric sections and trenches made for OSL sampling are indicated in this profile. Note the difference in surface and bedrock elevation between the Malcombe palaeo-meander with respect to that of the younger and more proximal Roche d'Or palaeo-meander. The alluvial sediments of the Malcombe palaeo-meander sampled for OSL are located ~5 m below the palaeo-channel of the Roche d'Or palaeo-meander at the position of geoelectric section II. MAC, Malcombe palaeo-meander; RDO, Roche d'Or palaeo-meander.

Table 1 Results of OSL dating. Measurement of dose rate relevant elements (K, Th, U) was carried out by high-resolution low-level gamma spectrometry at VKTA Rossendorf e.V. Dresden, Germany.

Sample	Moisture (%)	Water (%)	Grain size (μm)	*n*	Depth (m)	K (%)	Th (p.p.m.)	U (p.p.m.)	*D* (Gy ka^{-1})	D_e (Gy)	Age (ka)
MAC1-Q	19.1	20 ± 5	4–11	5	1.35	1.32 ± 0.07	15.60 ± 0.40	4.66 ± 0.16	3.80 ± 0.23	125.5 ± 1.0	33.0 ± 2.0
MAC2-Q	19.0	20 ± 5	4–11	5	1.35	1.38 ± 0.07	15.90 ± 0.40	5.08 ± 0.18	3.99 ± 0.25	107.8 ± 0.8	27.0 ± 1.7
MAC3-Q	21.0	20 ± 5	4–11	5	1.40	1.30 ± 0.07	18.20 ± 0.40	4.42 ± 0.16	3.93 ± 0.25	247.4 ± 2.7	63.0 ± 4.1
MAC4-Q	20.0	20 ± 5	4–11	5	1.40	1.25 ± 0.06	17.60 ± 0.40	4.72 ± 0.17	3.92 ± 0.25	375.9 ± 9.9	95.8 ± 6.5
RDO1-Q	17.2	20 ± 5	4–11	5	1.35	1.45 ± 0.04	14.70 ± 0.30	4.66 ± 0.22	3.69 ± 0.23	30.1 ± 0.5	8.16 ± 0.52
RDO2-Q	19.8	20 ± 5	4–11	12	1.35	1.47 ± 0.07	14.70 ± 0.50	5.02 ± 0.17	3.80 ± 0.25	25.1 ± 0.1	6.61 ± 0.43
RDO3-Q	17.1	20 ± 5	4–11	5	1.45	1.34 ± 0.07	14.30 ± 0.30	4.81 ± 0.18	3.61 ± 0.21	17.2 ± 0.1	4.77 ± 0.28
RDO4-Q	16.7	20 ± 5	4–11	7	1.45	1.30 ± 0.07	13.80 ± 0.50	4.66 ± 0.15	3.49 ± 0.23	16.9 ± 0.2	4.84 ± 0.32

n, number of aliquots.

Acknowledgements

The first author received funding by EL-TEM. We would like to thank the entire EUCOR-URGENT team at the University of Basel led by P. Ziegler. B. Regent and F. Souquière lent a strong helping hand during fieldwork. Reviews by S. Carretier, B. Nivière and associate editor J-F Ritz significantly improved the manuscript.

References

Becker, A., 2000. The Jura Mountains – an active foreland fold-and-thrust belt? *Tectonophysics*, **321**, 381–406.

Burkhard, M. and Sommaruga, A., 1998. Evolution of the western Swiss Molasse basin: structural relations with the Alps and the Jura belt. In: *Cenozoic Foreland Basins of Western Europe*. (A. Mascle, C. Puidgefàbregas, H.P. Luterbacher and M. Fernàndez eds), *Geol. Soc. Spec. Publ.* **134**, 279–298.

Chauve, P., Enay, R., Fluck, P. and Sittler, C., 1980. L'Est de la France (Vosges, Fossé Rhénan, Bresse, Jura). *Ann. Sci. Univ. Besançon*, **4**, 3–80.

Dreyfuss, M. and Glangeaud, L., 1950. La vallée du Doubs et l'évolution morphotectonique de la région bisontine. *Ann. Sci. Univ. Besançon*, **5**, 2–16.

Fejfar, O., Heinrich, W.-D. and Lindsay, E.H., 1998. Updating the Neogene rodent biochronology in Europe. *Meded. Ned. Inst. Toegepaste Geowet.*, **60**, 533–554.

Giamboni, M., Wetzel, A., Niviere, B. and Schumacher, M., 2004a. Plio-Pleistocene folding in the southern Rhinegraben recorded by the evolution of the drainage network (Sundgau area: northwestern Switzerland and France). *Eclogae Geol. Helv.*, **97**, 17–31.

Giamboni, M., Ustaszewski, K., Schmid, S.M., Schumacher, M.E. and Wetzel, A., 2004b. Plio-Pleistocene transpressional reactivation of Paleozoic and Paleogene structures in the Rhine-Bresse transform Zone (northern Switzerland and eastern France). *International Journal of Earth Sciences*, **93**, 207–223.

Guéllec, S., Mugnier, J.L., Tardy, M. and Roure, F., 1990. Neogene evolution of the western Alpine foreland in the light of ECORS data and balanced cross-sections. In: *Deep Structure of the Alps* (F. Roure, P. Heitzmann and R. Polino, eds). *Mém. Soc. Géol. Fr.*, **156**, 165–184.

Kastrup, U., Zoback, M.L., Deichmann, N., Evans, K.F., Giardini, D. and Michael, A.J., 2004. Stress field variations in the Swiss Alps and the northern Alpine foreland derived from inversion of fault plane solutions. *J. Geophys. Res.*, **109**, doi:10.1029/2003JB002550.

Kulig, G., 2005. *Erstellung einer Auswertesoftware zur Altersbestimmung mittels Lumineszenz-verfahren unter spezieller Berücksichtigung des Einflusses radioaktiver Ungleichgewichte in der 238U-Zerfallsreihe*. Unpublished BSc thesis, Universität Freiberg.

Laubscher, H., 1961. Die Fernschubhypothese der Jurafaltung. *Eclogae Geol. Helv.*, **54**, 222–282.

Locke, M.H. and Barker, R.D., 1995. Least-Squares deconvolution of apparent resistivity pseudosections. *Geophysics*, **60**, 1682–1690.

Madritsch, H., Schmid, S.M. and Fabbri, O., 2008. Interactions between thin- and thick-skinned tectonics at the northwestern front of the Jura fold-and-thrust-belt (eastern France). *Tectonics*, **27**, TC5005, doi:10.1029/2008TC002282.

Madritsch, H., Fabbri, O., Hagedorn, E.-M., Preusser, F., Schmid, S.M. and Ziegler, P.A. 2009. Feedback between erosion, uplift and active deformation: geomorphic constraints from the frontal Jura fold-and-thrust belt (eastern France). *Int. J. Earth. Sci. (Geol. Rundsch.)* (in press). doi:10.1007/s00531-009-0468-7

Mauz, B. and Lang, A., 2004. Removal of the feldspar-derived luminescence component from polymineral fine silt samples for optical dating applications: evaluation of chemical treatment protocols and quality control procedures. *Ancient TL*, **22**, 1–8.

Meyer, B., Lacassin, R., Brulhet, J. and Mouroux, B., 1994. The Basel 1356 earthquake: which fault produced it? *Terra Nova*, **6**, 54–63.

Mosar, J., 1999. Present-day and future tectonic underplating in the western Swiss Alps: reconciliation of basement/wrench-faulting and décollement folding of the Jura and Molasse basin in the Alpine foreland. *Earth Planet. Sci. Lett.*, **173**, 143–155.

Nivière, B. and Winter, T., 2000. Pleistocene northwards fold propagation of the Jura within the southern Upper Rhine Graben: seismotectonic implications. *Global Planet. Change*, **27**, 263–288.

Nivière, B., Giamboni, M., Innocent, C. and Winter, T., 2006. Kinematic evolution of a tectonic wedge above a flat-lying décollement: The Alpine foreland at the interface between the Jura Mountains (Northern Alps) and the Upper Rhine graben. *Geology*, **34**, 469–472.

Petit, C., Campy, M., Chaline, J. and Bonvalot, J., 1996. Major palaeohydrographic changes in Alpine foreland during the Pliocene-Pleistocene. *Boreas*, **25**, 131–143.

Pfiffner, O.A., Erard, P. and Stäuble, M., 1997. Two cross sections through the Swiss Molasse Basin (lines E4-E6, W1, W7-W10). In: *Deep structure of the Swiss Alps Results of NRP 20* (O.A. Pfiffner, P. Lehner, P. Heitzmann, S. Mueller and A. Steck, eds), pp. 64–72, Birkhäuser, Basel.

Preusser, F., 2004. Towards a chronology of the Late Pleistocene in the northern Alpine Foreland. *Boreas*, **33**, 195–210.

Schmid, S.M. and Slejko, D., 2009. Seismic source characterization of the Alpine foreland in the context of a probabilistic seismic hazard analysis by PEGASOS Expert Group 1 (EG1a). *Swiss J. Geosci.*, **102**, 121–148.

Simpson, G., 2004. Role of river incision in enhancing deformation. *Geology*, **32**, 341–344.

Ustaszewski, K. and Schmid, S.M., 2007. Latest Pliocene to recent thick-skinned tectonics at the Upper Rhine Graben - Jura Mountains junction. *Swiss J. Geosci.*, **100**, 293–312.

Willett, S.D. and Schlunegger, F. 2009. The last phase of deposition in the Swiss Molasse Basin: from foredeep to negative-alpha basin. *Basin Res.* (in press). doi:10.1111/j.1365-2117.2009.00435.x.

Wintle, A.G. and Murray, A.S., 2006. A review of quartz optically stimulated luminescence characteristics and their relevance in single-aliquot regeneration dating protocols. *Radiation Measurements*, **41**, 369–391.

Zeilinger, G., Schlunegger, F. and Simpson, G., 2005. The Oxaya anticline (northern Chile): a buckle enhanced by river incision? *Terra Nova*, **17**, 368–375.

Ziegler, P. and Fraefel, M., 2009. Response of drainage systems to Neogene evolution of the Jura fold-thrust belt and Upper Rhine Graben. *Swiss J. Geosci.*, **102**, 57–75.

Received 7 July 2009; revised version accepted 11 January 2010

Supporting Information

Supporting Information may be found in the online version of this article:

Table S1 Results of GPS leveling.

Please note: Wiley-Blackwell are not responsible for the content or functionality of any supporting materials supplied by the authors. Any queries (other than missing material) should be directed to the corresponding author for the article.

